Thermoresponsive Capsules: Hybrid Capsules via Self-Assembly of Thermoresponsive and Interfacially Active Bionanoparticle-Polymer Conjugates (Adv. Funct. Mater. 13/2011)

ARTICLE *in* ADVANCED FUNCTIONAL MATERIALS · JULY 2011

Impact Factor: 11.81 · DOI: 10.1002/adfm.201190049

ADVANCED FUNCTIONAL MATERIALS
www.afm-journal.de

www.MaterialsViews.com

Hybrid Capsules via Self-Assembly of Thermoresponsive and Interfacially Active Bionanoparticle–Polymer Conjugates

*Nathalie C. Mougin, Patrick van Rijn, Hyunji Park, Axel H. E. Müller, and Alexander Böker**

New bionanoparticles have been prepared from horse spleen ferritin by grafting thermoresponsive poly(*N*-isopropyl acrylamide) (PNIPAAm) and photo-crosslinkable *2*-(dimethyl maleinimido)-*N*-ethyl-acrylamide (DMIAAm) from the protein surface. The 72 addressable amino groups on the exterior of HSF were modified with *N*-hydroxysuccinimide-activated *2*-bromo-isobutyrate to form a macro-initiator for atom transfer radical polymerization, which was performed in water/DMF solutions at low temperature. The modification of the HSF and the presence of the polymer shell were confirmed by size exclusion chromatography (SEC), sodium dodecyl sulfate-polyacrylamide gel-electrophoresis, transmission electron microscopy, and scanning force microscopy. The thermoresponsive behavior of the ferritin-PNIPAAm conjugates was investigated in solution by UV–vis spectroscopy showing a phase transition in the form of a cloud point around 32 °C. Further, dynamic light scattering revealed an increasing hydrodynamic radius around this transition, indicating aggregation of the particles at elevated temperatures which was confirmed by transmission electron microscopy. Initial experiments show that the particles are highly surface active, much more than the individual components alone, which was demonstrated by pendant-drop interfacial tension measurements. This leads to the fact that they form stable Pickering emulsions, i.e., emulsion droplets decorated with polymer-modified bionanoparticles which can be cross-linked successively. This allows the formation of capsules with thermoresponsiveness for controlled release purposes, e.g., in drug delivery.

1. Introduction

The fabrication of functional nanoparticles and the control of their self-assembly has opened new opportunities for the bottom-up construction of functional nanostructured materials.[1] When making use of nanoparticles for these materials, one of the requirements is that the particles need to be monodisperse in size and introduce a certain functionality to the material. Proteins, protein assemblies, protein cages, and viruses are well defined monodisperse multifunctional bionanoparticles which are formed by controlled folding of peptide strands or self-assembly of several proteins, respectively.[2] Bionanoparticles have been modified with dyes, polymers, recognition sequences, drugs etc. by addressing different functionalities on the outer surface.[3–6] Their highly reproducible structure, precise positioning of functional groups, and monodispersity makes them perfect building blocks and scaffolds for the formation of well-defined nano-objects, e.g. quantum dots, nanotubes and -wires, or functional monolayers.[7–11] Horse spleen ferritin (HSF) has a very well characterized structure which is often used as a model protein cage. HSF is an iron storage protein in mammals and consists of a dodecameric protein cage of 12 nm in diameter with a 6 nm central cavity containing a phosphate ferrihydrite core. The protein cage is stable over a large pH range and temperatures up to 60 °C in water and can tolerate organic co-solvents. On the exterior, 72 chemically addressable primary amino-groups are located which were heretofore used for bioconjugation of dyes.[12–17] With respect to the increasing interest in bionanoparticles, polymer–protein conjugates are a versatile way of modifying proteins.[18–24] Especially in combination with a grafting-from approach via, e.g., ATRP,[25] a protein template gives access to a large variety of structures and ferritin is an excellent candidate in this regard.[26] PNIPAAm is a well-known thermoresponsive polymer exhibiting a LCST of 32 °C.[27,28] We previously developed the ATRP

Dr. N. C. Mougin, Dr. P. van Rijn, H. Park, Prof. A. Böker
DWI an der RWTH Aachen e.V.
Lehrstuhl für Makromolekulare Materialien und Oberflächen
RWTH Aachen University
Pauwelsstrasse 8, D-52056 Aachen, Germany
E-mail: boeker@dwi.rwth-aachen.de

Prof. A. H. E. Müller
Lehrstuhl für Makromolekulare Chemie II
Universität Bayreuth
D-95440 Bayreuth, Germany

DOI: 10.1002/adfm.201002315

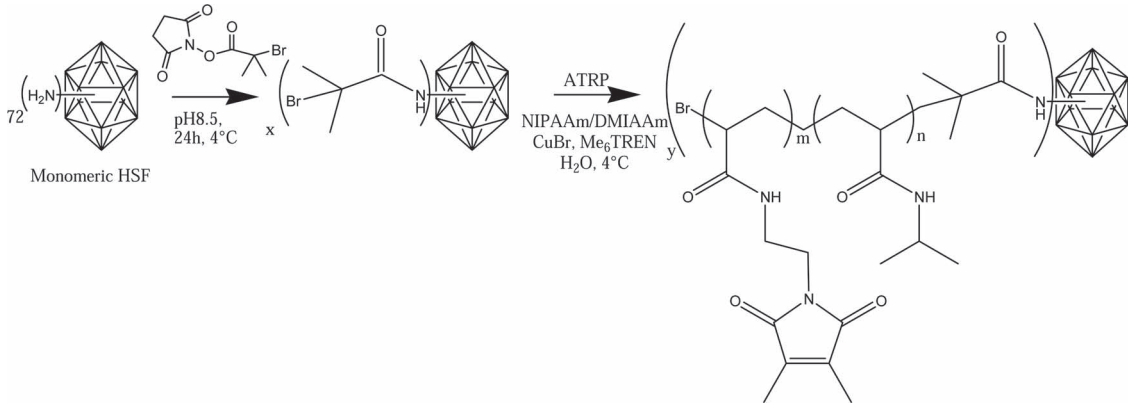

Scheme 1. Synthesis of the ferritin–BIBA macro-initiator (water/DMF, 5:1 v/v) followed by the random copolymerization of NIPAAm and DMIAAm, forming the ferritin-PNIPAAm–DMIAAm conjugates via ATRP in water.

of PNIPAAm in water at low temperatures[29,30] and envisaged extending this approach to the grafting of PNIPAAm from ferritin particles. Besides the formation of well defined protein–polymer structures, additional challenges remain with respect to the preparation of monomeric conjugates since aggregation of proteins may interfere with high monodispersity as ferritin tends to aggregate, and perturbs the control of the polymerization and the final structural features.

Here, we report on the successful synthesis of thermoresponsive ferritin–PNIPAAm and ferritin–PNIPAAm–DMIAAm conjugates via ATRP. Additionally, we present the thermoresponsive and interfacial behavior of these conjugates in aqueous solution. It was found that the newly formed bionanoparticles display a high surface activity at polar/apolar interfaces and can be used for stabilization of oil-in-water emulsions which allows for the formation of stable semi-permeable capsules by means of photo-crosslinking. In addition, the use of the supramolecular structures of the particles at interfaces, the polymer-conjugated ferritin particles may also find possible applications as functional conjugates with different cores for therapeutic and diagnostic purposes and with non-natural cores in the field of biomedical devices as delivery systems for anti-cancer, anti-microbial, or MRI contrast agents.[31–36] The combination of bionanoparticles like ferritin with responsive polymers like PNIPAAm is important with respect to size and reproducibility of the core structure with respect to synthetic inorganic nanoparticles and with potential catalytic activity when different bionanoparticles are to be used in the form of enzymes. The advantage of the biological aspect of the nanoparticle is the ability to mildly and selectively remove it by denaturation, leaving well defined empty spaces in self-assembled cross-linked polymer structures. This aspect increases the number of release mechanisms in formed capsules.

2. Results and Discussion

2.1. Modification of Ferritin

Ferritin was successfully transformed into a macro-initiator by attaching 2-bromo-isobutyric acid (BIBA) to the amino groups of the protein shell (**Scheme 1**). Analysis of the ferritin–BIBA conjugates with SEC and multi-angle laser light scattering showed that the particles remained intact and monomeric (see Supporting Information). It was found that the prepared ferritin solutions were stable up to 60 °C and in a pH-range from 3–9 at room temperature. By reaction with 5-carboxyfluorescein succinimidyl ester under conditions similar to the attachment of the initiator following a previously established protocol, the number of reacted amine groups was estimated to be at least 24 out of the 72 amine groups present on the outer surface.[37] The conditions reported earlier for the controlled polymerization of NIPAAm in aqueous solution with BIBA[29] were found to be well suited for the grafting of PNIPAAm and PNIPAAm–DMIAAm random copolymer from the protein surface via ATRP (Scheme 1).

Monomeric ferritin was stable under ATRP conditions. It is known that the copper used as transition metal catalyst in the polymerization can form a complex with the peptide bonds of the proteins.[38] However, this particular complexation was prevented by the addition of Me_6TREN, which is one of the strongest complexing agents. The addition of the catalyst solution to the protein solution is performed in such a way that the final catalyst concentration is very low. Using SEC, DLS, and TEM, no alterations in the protein size could be detected as a consequence of the polymerization conditions. That indeed a polymer shell grows around the bionanoparticles was shown by TEM and SFM (Figure 1 and 2). **Figure 1** shows single

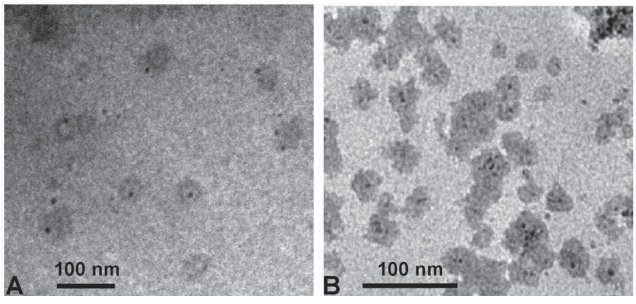

Figure 1. TEM images of A) Ferritin–PNIPAAm conjugates and B) Ferritin–$PNIPAAm_{95}$–$DMIAAm_5$ drop-cast from solutions with a concentration of ~4×10^{-6} mol L^{-1}.

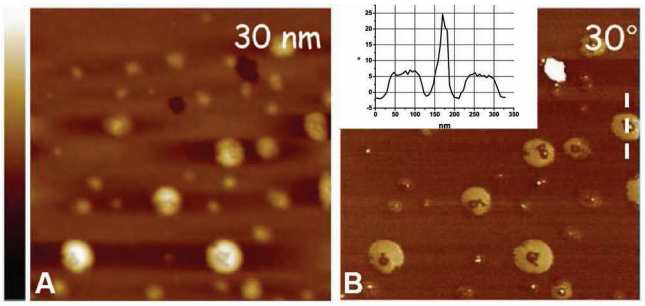

Figure 2. A) SFM topography (z = 30nm) and B) phase (z = 30°) images of horse spleen ferritin–PNIPAAm conjugates mixed with free ferritin prepared on a freshly cleaved mica sheet, over a 3 μm × 3 μm area. The iron oxide core of horse spleen ferritin appears as a white dot, the protein shell appears dark like the substrate background and the polymer shell is shown bright in the phase image. The inset displays the cross-section of a polymer–ferritin structure.

ferritin–PNIPAAm conjugates (A) and clustered ferritin–$PNIPAAm_{95}$–$DMIAAm_5$ conjugates (the subscript denotes the monomer ratios) (B). The iron core of ferritin has a high contrast in the TEM image and appears as a black dot of about 6 nm inside an area with less contrast depicting the polymer shell with a varying thickness. In both images, clustering is observed; this aggregation is attributed to a drying effect during sample preparation, leading to an increased concentration as well as a high tendency for adsorption onto the hydrophobic surface of the TEM grid. A more accurate diameter of the particle size is given by low concentration DLS measurements which will be discussed later.

For the SFM imaging, the solution of the bionanoparticle–polymer conjugates is mixed with monomeric ferritin, spread by drop casting on a freshly cleaved mica sheet and dried at room temperature to visualize the difference between the two entities in the image. At pH 7.5, mica sheets are hydrophilic and negatively charged, allowing a good adsorption of the proteins on the solid substrate (**Figure 2**). The ferritin–polymer conjugates appear in the height image (Figure 2A) as homogeneous dots of about 150 to 300nm in diameter (for a polymerization with a monomer:initiator ratio of 500:1). In the phase image (Figure 2B), the monomeric ferritins appear only as white dots of 6 nm because the phase information is related to the elastic response of the material and the hard iron core of ferritin results in a large phase shift. Thus, the phase image allows for discriminating between the soft protein cage (dark like the substrate), the hard iron core and the polymer shell (bright corona surrounding the dark protein cage).

2.2. Characterization of the Grafted Polymer Chains

Every polymerization was followed by ^{1}H NMR in D_2O using DMSO as internal standard. All polymerizations were completed to at least 90% within 24 h. Under the conditions of the NMR experiment, the signals of the protein were not observed. However, the disappearance of monomeric NIPAAm was followed by ^{1}H-NMR, analyzing the intensity of the peaks corresponding to the vinyl group at d = 5.72–5.80 ppm (dd, CH(H) =).

The molecular characterization of the polymer–ferritin conjugates imposes many challenges because of their high molecular weight. The denatured ferritin cage was investigated by SEC and MALDI–ToF MS. SEC of the denatured conjugates could not be measured in aqueous solution because PNIPAAm absorbs on the acrylamide column. The use of organic solvents (e.g., DMAc) prevents this, but it also alters the protein properties (conformation in solution) and the SEC measurements of the conjugates in dimethylacetamide yield non-satisfactory results. Moreover, SEC characterization of the conjugates depends on the polymer concentration, and on the refractive index increment of the protein/polymer mixture (d*n*/d*c*). It is quite difficult to evaluate dn/dc of the mixtures because it demands a high volume of conjugates. An alternative way to determine the molecular weight is to analyze free polymer chains from the addition of sacrificial initiator which was added to achieve a controlled polymerization reaction and allows for determining the polymer properties.[39] The characterization of free polymer chains is more accessible but due to the low amount it was only possible by MALDI–ToF MS and not by SEC. PNIPAAm with a low molecular weight, synthesized using ratios of monomer/initiator/Cu(I)/Cu(II)/ligand of 100/1/0.7/0.3/2, was successfully analyzed by MALDI–ToF MS and had a number average molecular weight (M_n) of 3.6 kDa and a PDI of 1.03 (see Supporting Information). With higher molecular weight PNIPAAm, the mass could no longer be detected by MALDI–ToF MS most likely due to poor matrix assisted ionization. The analysis of the free polymer provides an indirect proof of the progression of the polymerization reaction as well as an indication of what to expect with respect to the maximum length of the polymer chain.

2.3. Characterization of Ferritin–PNIPAAm and Ferritin–PNIPAAm–DMIAAm Conjugates

To prove that the polymers are indeed covalently attached to the ferritin, the polymer–bionanoparticle conjugates were denatured with 8 M urea and 10 mM dithiothreitol by heating to 90 °C for 3 min, and subjected to SDS–PAGE. The polypeptide subunit of ferritin has a molecular weight of 19–21 kDa depending on whether it is part of the light or heavy chain. However, the difference cannot be seen in the low resolution of the SDS–PAGE gel. The SDS–PAGE measurement in **Figure 3** shows that, after polymerization, no single subunit of monomeric ferritin is left which confirms that all of the 24 subunits were modified with at least one polymer chain.

The thermotropic transition of the conjugates was characterized by turbidity measurements at the nonspecific absorbance of 600 nm (see **Figure 4**). PNIPAAm undergoes an abrupt change in its dimensions at the LCST, followed by an aggregation of individual chains to larger particles, resulting in an optically detectable phase separation, i.e., a turbid solution. As the low molecular weight polymer derived from the sacrificial initiator was removed by dialysis, the conjugate solution turns turbid due to the phase transition of the covalently bound polymer. The detected cloud point of 32 ± 1°C is lower than the theoretical value of PNIPAAm alone; however, it depends on the molecular weight of the polymer.[40,41] Heating and cooling

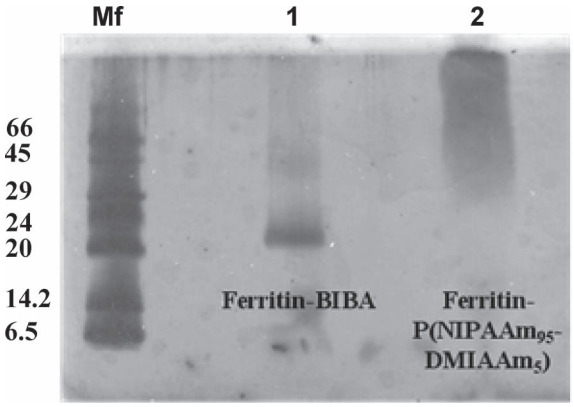

Figure 3. SDS–PAGE measurement of the macro-initiator ferritin–BIBA (1) and the conjugate ferritin–P(NIPAAm$_{95}$–DMIAAm$_5$) (2) after denaturing and staining with silver solution. (Mf is the reference marker).

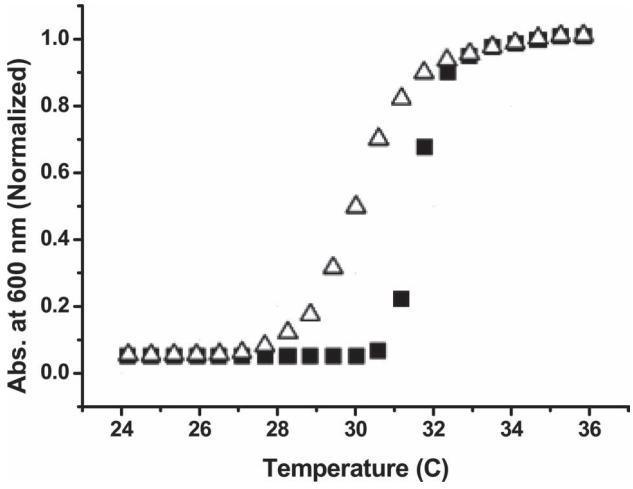

Figure 4. Turbidity measurement of the conjugates as function of temperature at a concentration of 4×10^{-6} mol L^{-1}. (■ heating cycle; Δ cooling cycle).

cycles prove that the conjugates are thermoresponsive as can be observed from Figure 4.

Dynamic light scattering measurements were also performed to investigate the behavior of the ferritin–PNIPAAm conjugates with increasing temperature from 20 to 40°C. The transition temperature, determined from the change in hydrodynamic radius due to the aggregation of the bioconjugates again was 32 ± 1°C. In **Figure 5**A, a decrease in the hydrodynamic radius was seen from 30 to 12 nm when raising the temperature from 20 to 32 °C. After further increasing the temperature, the hydrodynamic radius of the aggregates increased significantly. This may be explained by the increasing hydrophobicity of the collapsing PNIPAAm chains which tend to reduce their interface with water by first contracting and finally leading to aggregation of several conjugate particles. Transmission electron microscopy gives more insight into the behavior of the particles related to this phenomenon. While at 25 °C, non-aggregated and slightly aggregated particles were observed (Figure 5B), at 40 °C, large aggregates of 250 nm were identified (Figure 5C). The TEM images reveal aggregates of the collapsed PNIPAAm shells surrounded by the ferritin iron cores. We anticipate that quasi-amphiphilic particles are formed during the collapse of the polymer shell with ferritin as the hydrophilic part and PNIPAAm as the hydrophobic moiety.

2.4. Interfacial Properties of the Conjugates and Emulsion Stabilization

Initial results reveal that the conjugates display a strong preference for polar/apolar interfaces. Proteins are known to assemble at the liquid–gas and liquid–liquid interface, leading to a decrease of the interfacial tension; therefore they are used to stabilize emulsions and foams.[42] Ferritin–PNIPAAm conjugates have been investigated at a perfluorodecalin/water interface by dynamic pendant-drop interfacial tension measurements (**Figure 6**A). As references, the used buffer (Phosphate buffer: 0.15 M NaCl, 1.5 mM NaN_3, 9.8 mM KH_2PO_4, 15.2 mM K_2HPO_4) and solutions of PNIPAAm, pure ferritin, and the macro-initiator ferritin–BIBA particles in buffer were also investigated. The reference samples decrease the interfacial tension with time from 58 to 43 mN m^{-1} but they do not achieve equilibrium after 3000s. On the other hand, the ferritin–PNIPAAm conjugates reached equilibrium after 500 s and decreased the interfacial tension down to 20mN m^{-1} at equal concentration (Figure 6A). This strong effect may be explained by the high

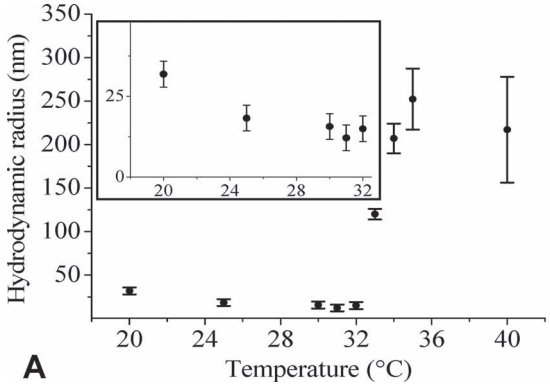

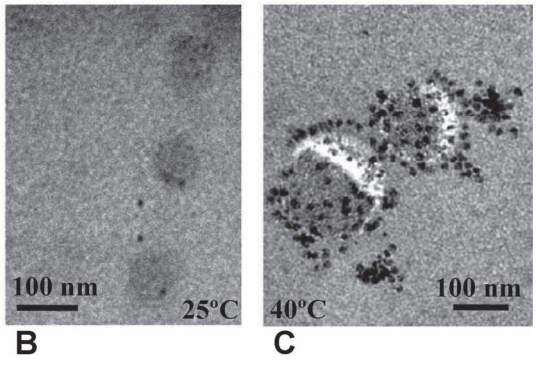

Figure 5. Effect of temperature on conjugate particles in solution at a concentration of 4×10^{-9} mol L^{-1}; A) DLS measurement of ferritin–PNIPAAm conjugate particles and TEM images of ferritin–polymer conjugates at B) 25 °C and C) after heating to 40 °C.

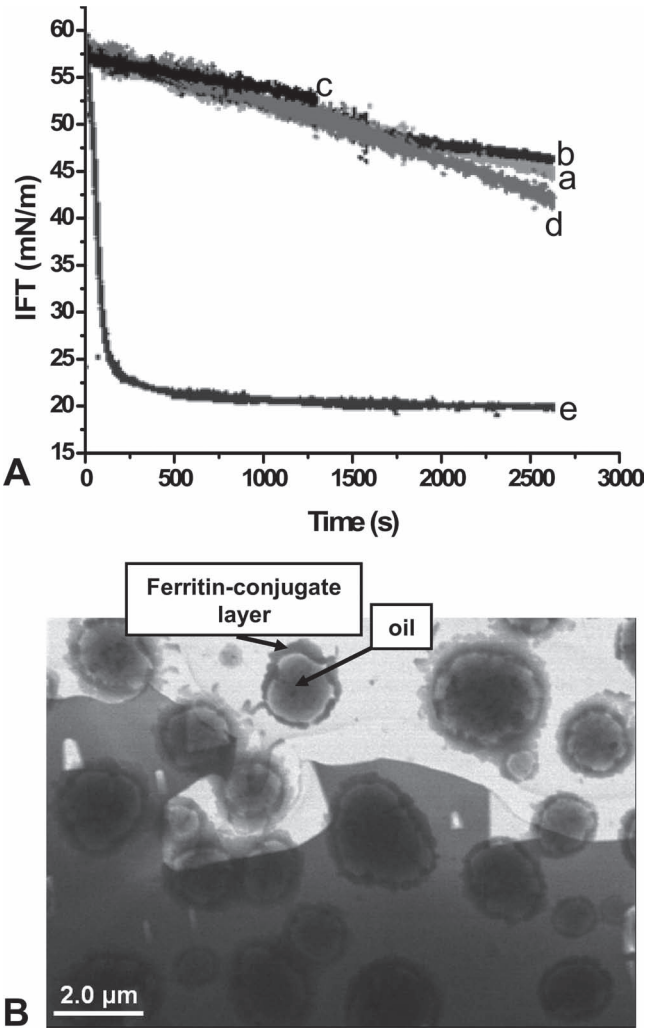

Figure 6. A) Dynamic pendant-drop interfacial tension measurements of a perfluorodecalin (PFD) drop in (a) pure phosphate buffer and (b) solutions of ferritin, (c) ferritin–BIBA, (d) PNIPAAm as references, and (e) the conjugates ferritin–PNIPAAm in phosphate buffer at pH 7.4 at equal concentration (~4×10^{-3} mg mL^{-1}). B) Cryo-TEM of ferritin–PNIPAAm/PFD capsules at a concentration of 7×10^{-3} mg mL^{-1} in pure water.

mobility of the PNIPAAm chains grafted from the ferritin possibly avoiding contact with the oil phase, leading to an enhanced amphiphilicity of the protein–polymer conjugates. The segregation of the conjugates to the polar/apolar interface can be clearly seen in Figure 6B. The cryo-TEM image displays an oil-in-water emulsion stabilized by ferritin–PNIPAAm. A shell of self-assembled conjugates is seen around the oil droplet. The shell thickness was found to be about 180 ± 50 nm by a statistical analysis of 100 data points at different positions distributed over various individual droplets. From DLS at 20 °C, it was found that the diameter of a single ferritin conjugate should be around 60 nm (twice the hydrodynamic radius) which means that the thickness corresponds to about 3 layers of conjugates around the oil droplet. However, the number of layers could be higher since the ferritin conjugate cannot be considered as a hard sphere and can be compressed, leading to a larger number of layers. The standard deviation of 50 nm is relatively large. In general, it was observed that small droplets have thinner conjugate layers around them (about 90–120 nm) than larger droplets (up to 300–350 nm). These findings suggest that preparing a more monodisperse emulsion would be beneficial for the polydispersity of the thickness of conjugate layer and that, by using smaller droplets, the conjugate layer would be driven more towards a monolayer. The surface active characteristics make the protein–polymer conjugates very good candidates for the stabilization of emulsions and an in-depth investigation of the surface activity and emulsion stabilization will be presented in future work.

In addition to stabilization of emulsions due to the interfacial activity of the conjugates, it was also possible to further stabilize ferritin–PNIPAAm–DMIAAm emulsions by photo-crosslinking. First an oil-in-water emulsion was prepared by mixing Benzotrifluoride (BTF), containing Nile Red as a fluorescent dye to visualize the oil phase by fluorescence microscopy, with the aqueous solution containing the ferritin–PNIPAAm–DMIAAm conjugate. The formed emulsion was then irradiated for 20 min with UV light which initiates a [2+2]-photocyclization of the DMIAAm moieties. The formed droplets are clearly visible as red spheres (**Figure 7**A) with an average diameter of 10 μm ± 3 μm (see Supporting Information). Then one volume equivalent of ethanol was added to the emulsion, which is known to break Pickering emulsions by mixing the oil and water phases. In the case of the control emulsion of non-crosslinked ferritin–PNIPAAm, the emulsion broke after addition of ethanol. However, as is observed from Figure 7B, the capsules stabilized via crosslinking of the protein–polymer conjugates remain intact and exhibit a dark capsule interior while the Nile Red is partially trapped in the capsule wall and the capsules analyzed have a diameter of of 28 μm ± 6 μm (see Supporting Information). It shows that the capsules are permeable to small molecules and that they can endure large osmotic pressures without being destroyed. From the analysis of the average diameter, it seems that the capsules swell after the addition of ethanol. However, due to high movement of the capsules and strong dilution, it cannot be said with great certainty. Finally, after drying of the sample, conjugate-based capsules could be found as shown in Figure 7C.

3. Conclusion

We achieved the synthesis of monomeric ferritin–PNIPAAm and ferritin–PNIPAAm–DMIAAm conjugates by ATRP in water at low temperatures. The polydispersity was highly reduced by purifying ferritin by SEC, obtaining monomeric ferritin particles. The modification of monomeric ferritin into a macro-initiator, followed by ATRP of NIPAAm and DMIAAm in water, results in well-defined protein–polymer conjugates. The polymer shell collapses around ferritin upon increasing the temperature. Above the LCST of 32 °C, aggregates of ferritin–PNIPAAm conjugates are formed, as visualized by TEM. The ferritin–PNIPAAm conjugates are interesting building blocks with responsive properties and display high interfacial activity at oil/water interfaces. This leads to for possible applications as emulsion stabilizers. Moreover, in combination with

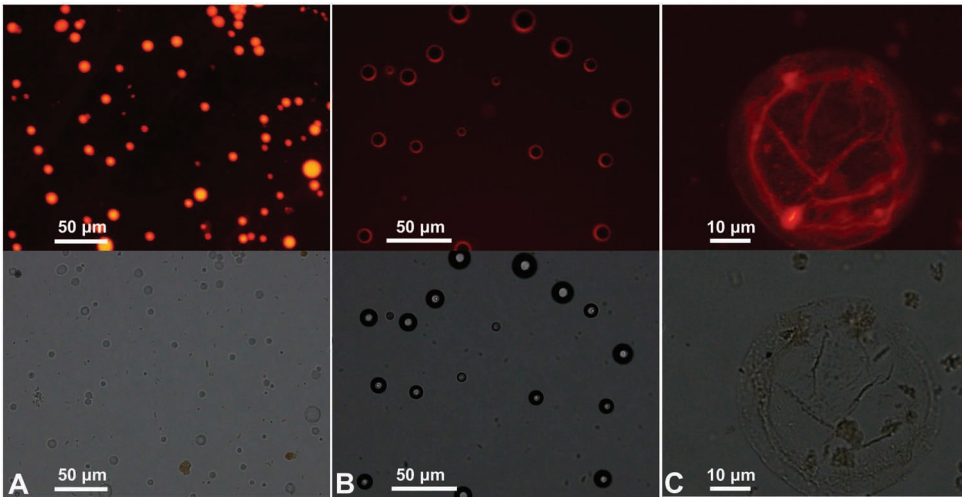

Figure 7. Fluorescence and light micrographs of A) emulsions of BTF/Nile Red in water stabilized by ferritin–PNIPAAm–DMIAAm conjugates (~1 mg mL^{-1}) and cross-linked by UV; B) after washing with ethanol; C) dried protein–polymer conjugate capsule.

cross-linking, stable capsules were formed which may be of use as delivery systems for (bio-)medical applications.

4. Experimental Section

Horse Spleen ferritin was purchased from Fluka. Dichloromethane was distilled over CaH_2 and stored under nitrogen. *2*-Bromoisobutyric acid (BIBA) (99%, Aldrich), *N*-hydroxysuccinimide (NHS) (Aldrich, 98%), *1,3*-dicyclohexal carbodiimide (DCC) (Aldrich, 99%) and DMF (peptide grade, Biotech) were used as purchased. NIPAAm (99%, Aldrich) was purified by two successive recrystallizations in a mixture of n-hexane and benzene (4:1 v:v). CuBr (98%, Aldrich) was purified by stirring in acetic acid overnight. After filtration, it was washed with ethanol and ether and then dried in vacuum, $CuBr_2$ (99%, Aldrich) was used as purchased. Me_6TREN was prepared as described by Ciampolini.[43] The photo-crosslinker monomer *2*-(dimethyl maleinimido)-*N*-ethyl-acrylamide (DMIAAm) was synthesized according to the procedure reported by Kuckling et al.[44] UV irradiation of the cross-linker was carried out with a 400W UV lamp (Panacol 400F), with emitting light with λ: 315–400 nm.

Preparation of Ferritin Macro-Initiator: *N*-hydroxysuccinimidyl *2*-bromo-isobutyrate (NHS-BIBA) was prepared according to Lecolley et al.[45] Ferritin was fractionated by aqueous SEC in 0.1M phosphate buffer at pH 8.0 (flow rate 0.250 mL min^{-1}) to obtain the non-aggregated monomeric fraction (see Supporting Information)[46]. The ferritin concentration was determined by the absorption at 280 nm ($\varepsilon_{280} = 4.8 \times 10^5$ M^{-1} cm^{-1}). The ferritin macro-initiator was prepared as previously communicated by Zeng et al.[37] A 500 fold excess of NHS-BIBA with respect to the 72 addressable amino groups per ferritin particles was used to ensure stoichiometric conversion. The reaction mixture in buffer:DMF (5:1 v/v) was then incubated for 12 hours at 4 °C. To remove excess initiator, the solution was dialyzed (cut-off value 14 kDa) in 0.1 M phosphate buffer at pH 7.4.

Preparation of Ferritin–PNIPAAm Conjugate: ATRP of NIPAAm was performed with a ratio: monomer/initiator/Cu(I)/Cu(II)/ligand = 100/1/0.7/0.3/2. The total amount of initiator was fixed at 4×10^{-6} mol, corresponding to the total amount of initiator moieties on ferritin and sacrificial initiator (BIBA). Sacrificial initiator is added to allow for a faster and more controlled polymerization process and for analysis of the polymer.[39] The dialyzed ferritin macro-initiator was shaken with NIPAAm and BIBA until complete dissolution. The sacrificial initiator was added afterwards to increase the amount of initiator up to 4×10^{-6} mol in the solution. In a second flask, CuBr, $CuBr_2$, and Me_6TREN were mixed, and dissolved in Millipore water. Both solutions were then degassed for 15 min in an ice bath. 0.5 mL of the copper/ligand solution was added to the ferritin solution under agitation. The polymerization was performed over 24 h to ensure a higher degree of polymerization. The reaction mixture was extensively dialyzed against 0.1 M phosphate buffer at pH 7.4 to remove the catalyst (cut-off 1kDa). Then the ferritin–PNIPAAm conjugate solution was dialyzed with a higher cut-off membrane (50 kDa) to remove the polymer formed by the sacrificial initiator. The same procedure was used for the copolymerization of the photo-crosslinkable monomer *2*-(dimethyl maleinimido)-*N*-ethyl-acrylamide (DMIAAm). Here both monomers, NIPAAm and DMIAAm, where mixed in a ratio of 95:5 and used in a random copolymerization reaction.

Ferritin–PNIPAAm and ferritin–PNIPAAm–DMIAAm conjugates were characterized by size exclusion chromatography (SEC) using a RI and UV (d = 270 nm) detection in 0.05 M solution of LiBr in dimethylacetamide (DMAc) as eluent with an elution rate of 0.72 mL min^{-1}. PSS GRAM columns (300 mm × 8 mm, 7 mm): 10^3, 10^2 Å (PSS) were thermostated at 70 °C and calibrated with polystyrene standards. ^{1}H-NMR spectra were recorded on a Bruker AC-25 spectrometer (300 MHz) in D_2O at room temperature. DMSO is used as internal standard to follow the monomer conversion.

TEM measurements were performed on a Zeiss Libra plus machine, operating at 120 kV. For cryo-TEM, images were taken using a Hitachi S-4800 field emission scanning electron microscopy (FESEM) instrument in the TE mode operating at 30 kV and 10 µA current.

Supporting Information

Supporting Information is available from the Wiley Online Library or from the author.

Acknowledgements

This project is financially supported by the EU Marie Curie RTN "BioPolySurf" and the Lichtenberg program of the VolkswagenStiftung. We thank Pierre-Eric Millard for his help with the development of the ATRP of PNIPAAm in water.

Received: December 3, 2010
Revised: January 11, 2011
Published online: March 28, 2011

[1] a) J. L. West, N. J. Halas, *Annu. Rev. Biomed. Eng.* **2003**, *5*, 285–292; b) A. G. Tkachenko, H. Xie, D. Coleman, W. Glomm, J. Ryan, M. F. Anderson, S. Franzen, D. L. Feldheim, *J. Am. Chem. Soc.* **2003**, *125*, 4700–4701; c) H. Bönnemann, R. M. Richards, *Eur. J. Inorg. Chem.* **2001**, *10*, 2455–2480.
[2] J. Spatz, S. Mössmer, C. Hartmann, M. Möller, T. Herzog, M. Krieger, H. G. Boyen, P. Ziemann, B. Kabius, *Langmuir* **2000**, *16*, 407–415.
[3] C. M. Niemeyer, *Angew. Chem. Int. Ed.* **2001**, *40*, 4128–4158.
[4] Y. Lin, A. Böker, J. B. He, K. Sill, H. Q. Xiang, C. Abetz, X. Li, J. Wang, T. Emrick, S. Long, Q. Wang, A. Balazs, T. P. Russell, *Nature* **2005**, *434*, 55–59.
[5] A. MaHam, Z. Tang, H. Wu, J. Wang, Y. Lin, *Small* **2009**, *5*, 1706–1721.
[6] M. Tominaga, M. Matsumoto, K. Soejima, I. Taniguchi, *J. Colloid Interface Sci.* **2006**, *299*, 761–765.
[7] I. Yamashita, *Thin Solid Films* **2001**, *393*, 12–18.
[8] H. Yoshimura, *Colloids Surf., A* **2006**, *282*, 464–470.
[9] J. M. Bonard, P. Chauvin, C. Klinke, *Nano Lett.* **2002**, *2*, 665–667.
[10] S. C. Tsang, J. S. Qiu, P. J. F. Harris, Q. J. Fu, N. Zhang, *Chem. Phys. Lett.* **2000**, *322*, 553–560.
[11] Y. Zhang, Y. Li, W. Kim, D. Wang, H. Dai, *Appl. Phys. A: Mater. Sci. Process.* **2002**, *74*, 325–328.
[12] K. Wetz, R. Crichton, R.*Eur. J. Biochem.* **1976**, *61*, 545–550.
[13] J. L. Farrant, *Biochim. Biophys. Acta* **1954**, *13*, 569–576.
[14] S. Silk, E. Breslow, E.*J. Biol. Chem.* **1976**, *251*, 6963–6973.
[15] W. Mainwari, T. Hoffmann, T.*Arch. Biochem. Biophys.* **1968**, *125*, 975.
[16] a) J. M. Hannink, J. J. L. M. Cornelissen, J. A. Farrera, P. Foubert, F. C. De Schryver, N. A. J. M. Sommerdijk, R. J. M. Nolte, *Angew. Chem. Int. Ed.* **2001**, *40*, 4732–4734; b) F. C. Meldrum, B. R. Heywood and S. Mann, *Science* **1992**, *257*, 522–523; c) S. Aime, L. Frullano, S. Geninatti Crich, *Angew. Chem.* **2002**, *114* (6) 1059–1061; d) O. Kasyutich, A. Ilari, A. Fiorillo, D. Tatchev, A. Hoell, P. Ceci, *J. Am. Chem. Soc.* **2010**, *132*, 3621–3627.
[17] Q. Zeng, R. Reuther, J. Oxsher, Q. Wang, *Bioorg. Chem.* **2008**, *36*, 255–260.
[18] D. Bontempo, K. L. Heredia, B. A. Fish, H. D. Maynard, *J. Am. Chem. Soc.* **2004**, *126*, 15372–15373.
[19] J.-F. Lutz, H. G. Börner, K. Weichenhan, *Macromolecules* **2006**, *39*, 6376–6383.
[20] Q. Wang, K. S. Raja, K. D. Janda, T. Lin, M. G. Finn, *Bioconjugate Chem.* **2003**, *14*, 38–43.
[21] J. Nicolas, V. San Miguel, G. Mantovani, D. M. Haddleton, *Chem. Commun.* **2006**, *45*, 4697–4699.
[22] S. Venkataraman, K. L. Wooley, *Macromolecules* **2006**, *39*, 9661–9664.
[23] H. G. Börner, *Macromol. Chem. Phys.* **2007**, *208*, 124–130.
[24] L. Albertin, M. H. Stenzel, C. Barner-Kowollik, L. J. R. Foster, T. P. Davis, *Macromolecules* **2005**, *38*, 9075–9084.
[25] P.-E. Millard, N. C. Mougin, A. Böker, A. H. E. Müller, *Polym. Prepr. Am. Chem. Soc., Div. Polym. Chem.* **2008**, *49*, 121.
[26] a) S. Edmondson, V. L. Osborne, W. T. S. Huck, *Chem. Soc. Rev.* **2004**, *33*, 14–22; b) J. Nicolas, G. Mantovani, D. M. Haddleton, *Macromol. Rapid Commun.* **2007**, *28*, 1083–1111; c) Y. Hu, D. Samanta, S. S. Parelkar, S. W. Hong, Q. Wang, T. P. Russell, T. Emrick, *Adv. Funct. Mater.* **2010**, *20*, 3603–3612.
[27] S. Fujishige, K. Kubota, I. Ando, *J. Phys. Chem.* **1989**, *93*, 3311–3313.
[28] H. G. Schild, *Prog. Polym. Sci.* **1992**, *17*, 163.
[29] P.-E. Millard, N. C. Mougin, A. Böker, A. H. E. Müller, *Controlled/Living Radical Polymerization: Progress in ATRP, ACS Symp. Ser.* **2009**, *1023*, 127–139.
[30] K. Matyjaszweski, J. H. Xia, *Chem. Rev.* **2001**, *101*, 2921–2990.
[31] K. S. Raja, Q. Wang, M. J. Gonzalez, M. Manchester, J. E. Johnson, M. G. Finn, *Biomacromolecules* **2003**, *4*, 472–476.
[32] B. Lele, H. Murata, K. Matyjaszewski, A. J. Russell, *Biomacromolecules* **2005**, *6*, 3380–3387.
[33] D. Bontempo, R. C. Li, T. Ly, C. Brubaker, H. D. Maynard, *Chem. Commun.* **2005**, 4702–4704.
[34] K. L. Heredia, D. Bontempo, T. Ly, J. T. Byers, S. Halstenberg, H. D. Maynard, *J. Am. Chem. Soc.* **2005**, *127*, 16955–16960.
[35] R. M. Broyer, G. M. Quaker, H. D. Maynard, *J. Am. Chem. Soc.* **2008**, *130*, 1041–1047.
[36] N. C. Mougin, A. H. E. Müller, A. Böker, *Polym. Mater. Sci. Eng.* **2008**, *99*, 713.
[37] Q. B. Zeng, T. Li, B. Cash, S. Q. Li, F. Xie, Q. Wang, *Chem. Commun.* **2007**, 1453–1455.
[38] P. K. Smith, R. I. Krohn, G. T. Hermanson, A. K. Mallia, F. H. Gartner, M. D. Frovenzano, E. K. Fujimoto, N. M. Goeke, B. J. Olson, D. C. Klenk, *Anal. Biochem.* **1985**, *19*, 76–85.
[39] J. Pyun, K. Matyjaszewski, *Chem. Mater.* **2001**, *13*, 3436–3448.
[40] H. D. Maynard, K. L. Heredia, R. C. Li, D. P. Parra, V. Vazquez-Dorbatt, *J. Mater. Chem.* **2007**, *17*, 4015–4017.
[41] C. M. Schilli, A.H. E. Müller, E. Rizzardo, S. H. Thang, Y. K. Chong, *Advances in Controlled/Living Radical Polymerization, ACS Symp. Ser.* **2003**, *854*, 603–618.
[42] a) E. Dickinson, *Soft Matter* **2008**, *4*, 932–942; b) S. Damodaran, *J. Food Sci.* **2005**, *70*, R54–R66; c) B. S. Murray, *Curr. Opin. Colloid Interface Sci.* **2007**, *12*, 232–241; d) J. T. Russell, Y. Lin, A. Böker, L. Su, P. Carl, H. Zettl, J. He, K. Sill, R. Tangirala, T. Emrick, K. Littrell, P. Thiyagarajan, D. Cookson, A. Fery, Q. Wang, T. P. Russell, *Angew. Chem. Int. Ed.* **2005**, *44*, 2420.
[43] M. Ciampolini, Nardi, N.*Inorg. Chem.* **1966**, *5*, 41.
[44] L. Ling, W. D. Habicher, D. Kuckling, H.-J. Adler, *Des. Monomers Polym.* **1999**, *4*, 351–358.
[45] F. Lecolley, L. Tao, G. Mantovani, I. Durkin, S. Lautru, D. M. Haddleton, *Chem. Commun.* **2004**, 2026–2027.
[46] P. Aisen, I. Listowsky, *Ann. Rev. Biochem.* **1980**, *49*, 357–393.